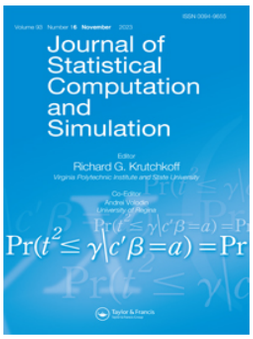

Journal of Statistical Computation and Simulation

ISSN: (Print) (Online) Journal homepage: https://www.tandfonline.com/loi/gscs20

An adaptive max-type multivariate control chart by considering measurement errors and autocorrelation

Hamed Sabahno

To cite this article: Hamed Sabahno (2023) An adaptive max-type multivariate control chart by considering measurement errors and autocorrelation, Journal of Statistical Computation and Simulation, 93:16, 2956-2981, DOI: 10.1080/00949655.2023.2214830

To link to this article: https://doi.org/10.1080/00949655.2023.2214830

Published online: 04 Jun 2023.

JOURNAL OF STATISTICAL COMPUTATION AND SIMULATION
2023, VOL. 93, NO. 16, 2956–2981
https://doi.org/10.1080/00949655.2023.2214830

Taylor & Francis
Taylor & Francis Group

An adaptive max-type multivariate control chart by considering measurement errors and autocorrelation

Hamed Sabahno

Department of Statistics, School of Business, Economics and Statistics, Umeå University, Umeå, Sweden

ABSTRACT

The combined effect of two real-world-occurring phenomena: 'measurement errors' and 'autocorrelation between observations' has rarely been investigated. In this paper, it will be investigated for the first time on 'adaptive' and/or 'simultaneous monitoring' charts and also for the first time by using the multivariate linearly covariate measurement errors and VARMA (vector mixed autoregressive and moving average) autocorrelation models, and Markov chains-based performance measures. In addition, this paper for the first time proposes a skip-sampling strategy in an ARMA/VARMA model for alleviating the autocorrelation effect. To do so, we add the above-mentioned measurement errors and autocorrelation models to a recently developed adaptive max-type chart. Then, we develop a Markov chain model to compute the performance measures. After that, extensive numerical analyses will be performed to investigate their combined effect as well as some methods to alleviate their negative effects. Finally, an illustrative example involving a real industrial case will be presented.

ARTICLE HISTORY
Received 7 July 2022
Accepted 12 May 2023

KEYWORDS
Multivariate control charts; adaptive control charts; max-type control charts; measurement errors; autocorrelation; Markov chains

1. Introduction

Control charts, the main tool of SPC (statistical process control), can be used to reduce process variability as well as to ensure the delivery of good quality products/services. If the product/service consists of more than one quality characteristic ($p > 1$), the multivariate control charts should be employed for process monitoring. Classical control charts are slow in detecting assignable causes that lead to small or moderate shifts. A common way of addressing this issue is to use adaptive control charts. By doing so, the charts' parameters are allowed to vary during online process monitoring. The best adaptive approach is by allowing all the chart's parameters (i.e. sample size, sampling interval, and control limits) to vary, namely the variable parameters (VP) scheme [1]. Faraz et al. [2], Seif et al. [3], and Sabahno et al. [1,4,5] are among the researchers who considered the VP adaptive feature on the multivariate control charts. For other types of adaptive features contributed to multivariate control charts, one can refer to Lee and Khoo [6] and Sabahno et al. [1,7,8].

CONTACT Hamed Sabahno hamed.sabahno@umu.se Department of Statistics, School of Business, Economics and Statistics, Umeå University, 90187, Umeå, Sweden

Moreover, monitoring the process parameters simultaneously is known to reduce the false alarm rate and improve the performance of the control chart. Simultaneous monitoring of the mean and variability parameters by control charts can be considered in single- or double-chart schemes. Single-chart ones are easier to administer. Yeh et al. [9] and Reynolds and Gyo-Young [10] are among those who studied multivariate double-chart schemes. Khoo [11], Zhang et al. [12], and Wang et al. [13] have contributed to multivariate single-chart schemes. Reynolds and Kim [14] and Reynolds and Cho [15] added adaptive features to multivariate double-chart schemes and Sabahno et al. [1,4,5], Sabahno and Khoo [16], Sabahno and Amiri [17], to multivariate single-chart schemes. For more information regarding different simultaneous monitoring schemes, we refer interested researchers to Jalilibal et al. [18].

In the real world, regardless of how advanced the measurement system is, the process is faced with measurement errors on some level. It has been shown that measurement errors deteriorate the chart's performance. Evaluating the effect of measurement errors on different control charts is of growing interest to researchers. Among different measurement errors models, the linear covariate model introduced by Linna and Woodall [19], which is an extension of the simple linear additive model, is the most common one. Linna et al. [20], Chattinnawat and Bilen [21], and Zaidi et al. [22] considered measurement errors in Hotelling's T^2 control charts for monitoring the mean vector, and Huwang and Hung [23] have done the same to monitor the variance-covariance matrix. Sabahno et al. [7,8] considered the measurement errors' effect on two different adaptive Hotelling's T^2 control charts. Sabahno et al. [4], Khati Dizabadi et al. [24], and Ghashghaei et al. [25] are examples of researchers who considered the measurement errors' effect in simultaneous monitoring using control charts. For more information regarding the effect of measurement errors on different control charts, we refer interested researchers to Maleki et al. [26].

In real applications, a commonly occurring phenomenon is autocorrelation among consecutive observations, which mainly occurs due to fast consecutive measurements. One of the most common autocorrelation models is the mixed autoregressive and moving average (ARMA) model, which is a general form of the simpler autocorrelation models: autoregressive (AR) and moving average (MA).

Several studies have shown that autocorrelation in the process can deteriorate the chart's performance. Interesting papers regarding the investigation of autocorrelation effect on the multivariate control charts have been published by Kalgonda and Kulkarnin [27], Jarrett and Pan [28], Vanhatalo and Kulahci [29], Leoni et al. [30], Dargopatil and Ghute [31], Sabahno et al. [5], and Rahimi et al. [32,33].

Costa and Castagliola [34] introduced the skip-sampling method to alleviate the autocorrelation effect in a univariate $\bar{\mathbf{X}}$ control chart with a AR model of order (1), AR (1). Franco et al. [35] proposed another sampling strategy for a $\bar{\mathbf{X}}$ control chart with a AR (1) autocorrelation model, by mixing the current and previous samples (instead of skipping observations during the current sampling) and showed that their strategy performs only on some limited situations better than the skip-sampling strategy. Franco et al. [36] considered the economic-statistical design of the $\bar{\mathbf{X}}$ control charts. They used the AR (1) autocorrelation model and implemented the skip-sampling strategy. Ma et al. [37] introduced the sequential skipping strategy for individual observations and used a model-free approach in three different control charts ($\bar{\mathbf{X}}$, Hotelling's T^2 and PCA-based control charts). All these

researchers have proposed alleviating strategies based on positive autocorrelations, which is actually a more common case in industrial practice.

A more realistic phenomenon in any process is that it contains both measurement errors and autocorrelation together. However, only four papers that investigated their combined effect on the univariate control charts could be found, and only one on the multivariate control charts. Yang and Yang [38] were the first to investigate the combined effect of measurement errors and autocorrelation on a univariate Shewhart control chart. They used an ARMA (1) autocorrelation model and a simple additive measurement errors model. Xiaohong and Zhaojun [39] investigated such an effect on a univariate CUSUM control chart, this time with a AR (1) autocorrelation model. Costa and Castagliola [34] investigated this combined effect on a $\bar{\mathbf{X}}$ control chart. They considered the AR (1) and simple additive measurement errors models. They used skip-sampling to alleviate the AR (1) autocorrelation effect and multiple measurements to alleviate the measurement errors effect. They used the simulation method to compute the performance measures. Shongwe et al. [40] investigated this combined effect on the synthetic and runs-rules univariate schemes and used the AR (1) autocorrelation and linearly covariate measurement errors models, and, for the first time used Markov chains to compute the average run length in such schemes. Beydaghi et al. [41] did exactly the same as Costa and Castagliola [34], but this time for a multivariate T^2 Hotelling control chart.

Based on the above paragraph, it is clear that there is a huge research gap in this area. In the case of univariate control charts, this combined effect has not been investigated on adaptive and/or simultaneous monitoring schemes. In addition, no strategy has been proposed to alleviate the autocorrelation effect, when the ARMA models are used. In the case of multivariate control charts, in which only one research could be found, other than the same gaps as in the univariate charts, the combined effect has not been investigated when the VARMA autocorrelation and/or linearly covariate measurement errors models are used.

> In this paper, we will fill all the above-mentioned research gaps by considering the combined effect of measurement errors and autocorrelation on a multivariate control chart with (i) a linearly covariate measurement errors model (instead of so far used simple linear model) (ii) a VARMA autocorrelation model (instead of so far used VAR model); with a skip-sampling strategy for ARMA/VARMA models, (iii) VP adaptive feature (instead of so far used fixed-parameter charts), (iv) simultaneous parameters monitoring (instead of so far used single process parameter (mean) monitoring), and, (v) Markov chains-based performance measures (instead of so far used simulation method). To do so, we add the linearly covariate measurement errors and VARMA (1,1) autocorrelation models to the recently developed adaptive control chart of Sabahno et al. [1] for simultaneously monitoring of the multivariate normal process parameters.

This paper is structured as follows: In Section 2, the linearly covariate measurement errors model with multiple measurements is introduced. In Section 3, the vector ARMA (VARMA) autocorrelation model is developed with a skip-sampling strategy. In Section 4, a max-type multivariate control chart with autocorrelation and measurement errors is proposed. Next, the adaptive features of the proposed control chart and their design procedure are discussed. In Section 5, Markov chains-based performance measures are developed. In Section 6, extensive simulation studies and numerical analyses are performed to investigate the combined effects of measurement errors and autocorrelation in different

scenarios. In Section 7, based on a real case, an example is illustrated to show how the proposed control chart can be implemented in real practice. Finally, concluding remarks and some suggestions for future research are discussed in Section 8.

2. Linearly covariate measurement errors model

There is usually a difference between the observed and true values in any process, depending on the measurement system and tools. Similar to Sabahno et al. [7,8], let us assume that $\mathbf{Y}_{ij}$ is a vector of p quality characteristics. Samples $j = 1,2,3,...,\ n$ are taken every $i = 1, 2, 3, \ldots$ time. We assumed that$\mathbf{Y}_{ij}$ follows a multivariate normal distribution $\mathrm{MN}(\mu_0, \mathbf{\Sigma}_0)$, where μ_0 is the known in-control mean vector and $\mathbf{\Sigma}_0$ is the known in-control variance-covariance matrix of the quality characteristics. It is also assumed that $\mathbf{Y}_{ij}$ is not directly observable and can only be assessed through $k = 1, \ldots, m$ measurements vectors $\mathbf{X}_{ijk}$ which is related to$\mathbf{Y}_{ij}$ using the following linearly covariate measurement errors model:

$$\mathbf{X}_{ijk} = \mathbf{A} + \mathbf{B}\mathbf{Y}_{ij} + \boldsymbol{\varepsilon}_{ijk}, \tag{1}$$

where $\mathbf{A}$ is a $p \times 1$ vector of constant values, $\mathbf{B}$ is a $p \times p$ diagonal matrix of constant values and $\boldsymbol{\varepsilon}_{ijk}$ is a $p \times 1$ vector of random measurement errors which is independent of $\mathbf{Y}_{ij}$ and is also assumed to follow a multivariate normal $\mathrm{MN}(\mathbf{0}, \mathbf{\Sigma}_{\boldsymbol{\varepsilon}})$ distribution, where $\mathbf{\Sigma}_{\boldsymbol{\varepsilon}}$ is the known variance-covariance matrix of measurement errors. Thereafter, $\mathbf{X}_{ijk}$ follows a multivariate normal $\mathrm{MN}(\mathbf{A} + \mathbf{B}\mu_0, \mathbf{B}\mathbf{\Sigma}_0\mathbf{B}^{\mathbf{T}} + \mathbf{\Sigma}_{\boldsymbol{\varepsilon}})$ distribution.

The sample mean vector $\bar{\mathbf{X}}_i$ for each sample ($i = 1,2,3, \ldots$) is computed as:

$$\bar{\mathbf{X}}_i = \frac{1}{mn} \sum_{j=1}^{n} \sum_{k=1}^{m} \mathbf{X}_{ijk}. \tag{2}$$

By substituting Equation (1) in Equation (2), we have:

$$\bar{\mathbf{X}}_i = \mathbf{A} + \mathbf{B}\bar{\mathbf{Y}}_i + \frac{1}{mn} \sum_{j=1}^{n} \sum_{k=1}^{m} \boldsymbol{\varepsilon}_{ijk}. \tag{3}$$

Since$\mathbf{Y}_{ij}$ and $\mathbf{X}_{ijk}$ are independent multivariate normal random variables, $\bar{\mathbf{X}}_i$ also follows a multivariate normal MN $(\mathbf{A} + \mathbf{B}\mu_0\ ,\mathbf{B}\mathbf{\Sigma}_{\bar{\mathbf{Y}}_0}\mathbf{B}^{\mathbf{T}} + (1/mn)\mathbf{\Sigma}_{\boldsymbol{\varepsilon}})$ distribution.

3. Varma autocorrelation model

In a sampling system in which the observations within a sample are collected very close in time, autocorrelation and cross-correlation among consecutive observations should be considered. To model autocorrelation, we assume that $\mathbf{Y}_t = (Y_{1,t}, Y_{2,t}, \ldots, Y_{p,t})'$: $t = 0, \pm 1, \pm 2, \pm 3, \ldots$, which as discussed in the previous section, follows a multivariate normal $\mathrm{MN}(\mu_0, \mathbf{\Sigma}_0)$ distribution.

One of the most common autocorrelation models is the VARMA model, which is obtained by combining the VAR and VMA models. For the VARMA model of order (1,1),

we have:

$$\mathbf{Y}_t - \mu_0 = \Phi(\mathbf{Y}_{t-1} - \mu_0) + \mathbf{e}_t - \Theta\mathbf{e}_{t-1}, \tag{4}$$

where $\mathbf{e}_t$, which follows a multivariate normal MN($\mathbf{0}$, $\mathbf{\Sigma}_e$), is a p-variate normal random noise vector, Φ is a $p \times p$ matrix of autoregressive coefficients (VAR component), and Θ is a $p \times p$ matrix of moving-average coefficients (VMA component). Note that if $\Phi = 0$ ($\Theta = 0$), the VARMA model changes into a VMA (VAR) autocorrelation model, and if $\Phi\&\Theta = 0$ it means that the observations are uncorrelated. Also, note that as opposed to the measurement errors case, in the case of autocorrelation the observed and true values of the quality characteristics are the same.

Two important properties of a VARMA autocorrelation model are stationarity and invertibility. To have the stationarity and invertibility conditions satisfied, the eigenvalues of the Φ and Θ matrices should be less than one in absolute value, respectively.

Sabahno et al. [5] showed that the covariance matrix $\mathbf{\Sigma}_0$ for the investigated multivariate process can be obtained as:

$$Vec\,\mathbf{\Sigma}_0 = (I_{p^2} - \Phi \otimes \Phi)^{-1} Vec\,\mathrm{A}, \tag{5}$$

where $\mathbf{A} = \Theta\mathbf{\Sigma}_{e_0}(\Theta' - \Phi') - \Phi\mathbf{\Sigma}_{e_0}\Theta' + \mathbf{\Sigma}_{e_0}$, $\mathbf{\Sigma}_{e_0}$ is the in-control value of $\mathbf{\Sigma}_e$, $\otimes$ is the Kronecker product operator, *Vec* is the operator that transforms a matrix into a vector by stacking its columns, and $\mathbf{I}_{p^2}$ is a $p^2 \times p^2$ identity matrix. Note that, if there is no autocorrelation, i.e. $\Phi = 0$ and $\Theta = 0$, then $\mathbf{\Sigma}_0 = \mathbf{\Sigma}_{e_0}$.

Again from Sabahno et al. [5], we have the variance-covariance matrix of the sample mean, $\mathbf{\Sigma}_{\bar{\mathbf{Y}}}$, equal to:

$$\begin{aligned}\mathbf{\Sigma}_{\bar{\mathbf{Y}}} = {} & \frac{1}{n}[\Gamma(0) + \Gamma(1)[(\Phi'2 - \Phi'n)[\Phi'(\mathbf{I} - \Phi')]^{-1} + \mathbf{I}] + [\Phi(\mathbf{I} - \Phi)^{-1} + \mathbf{I}]\Gamma(1)'] \\ & - \frac{1}{n^2}\big[\Gamma(1)[(\mathbf{I} - \Phi'n)(\mathbf{I} - \Phi')^{-2} - n\Phi'n - 1(\mathbf{I} - \Phi')^{-1} - 2\mathbf{I}] \\ & + [(\mathbf{I} - \Phi^n)(\mathbf{I} - \Phi)^{-2} - 2\mathbf{I}]\Gamma(1)'\big],\end{aligned} \tag{6}$$

where $\Gamma(0) = \mathbf{\Sigma_0}$ and $\Gamma(1) = \Gamma(0)\Phi' - \mathbf{\Sigma}_e\Theta'$. We also have: $\Gamma(-l) = \Gamma(l)'$ and $\Gamma(0) = E[(\mathbf{Y}_t - \mu_0)(\mathbf{Y}_t - \mu_0)']$.

Consequently, the sample mean $\bar{\mathbf{Y}}_i$ follows a multivariate normal MN(μ_0, $\Sigma_{\bar{\mathbf{Y}}_0}$) distribution. Note that, in the case of in-control process variability, we use $\mathbf{\Sigma}_{e_0}$ and in the case of out-of-control process variability, we use $\mathbf{\Sigma}_{e_1}$.

We now reconstruct the VARMA (1,1) autocorrelation model to be able to use the skip-sampling strategy. In a skip-sampling strategy, we skip $s = 0,1,2,3,\ldots$ observations while collecting a subgroup of n samples.

For $s = 1,2,3$, assuming $\tilde{\mathbf{Y}}_t = \mathbf{Y}_t - \mu_0$, Equation (4) changes into:

$$\begin{aligned}
\text{for } s = 1: \tilde{\mathbf{Y}}_t &= \Phi\tilde{\mathbf{Y}}_{t-1} + \mathbf{e}_t - \Theta\mathbf{e}_{t-1} = \Phi(\Phi\tilde{\mathbf{Y}}_{t-2} + \mathbf{e}_{t-1} - \Theta\mathbf{e}_{t-2}) + \mathbf{e}_t - \Theta\mathbf{e}_{t-1} \\
&= \Phi^2\tilde{\mathbf{Y}}_{t-2} + \mathbf{e}_t + (\Phi - \Theta)\mathbf{e}_{t-1} - \Phi\Theta\mathbf{e}_{t-2}, \\
\text{for } s = 2: \tilde{\mathbf{Y}}_t &= \Phi^2(\Phi\tilde{\mathbf{Y}}_{t-3} + \mathbf{e}_{t-2} - \Theta\mathbf{e}_{t-3}) + \mathbf{e}_t + (\Phi - \Theta)\mathbf{e}_{t-1} - \Phi\Theta\mathbf{e}_{t-2} \\
&= \Phi^3\tilde{\mathbf{Y}}_{t-3} + \Phi^2\mathbf{e}_{t-2} + \mathbf{e}_t + (\Phi - \Theta)\mathbf{e}_{t-1} + \Phi(\Phi - \Theta)\mathbf{e}_{t-2} - \Phi^2\Theta\mathbf{e}_{t-3}, \\
\text{for } s = 3: \tilde{\mathbf{Y}}_t &= \Phi^3(\Phi\tilde{\mathbf{Y}}_{t-4} + \mathbf{e}_{t-3} - \Theta\mathbf{e}_{t-4}) + \mathbf{e}_t \\
&\quad + (\Phi - \Theta)\mathbf{e}_{t-1} + \Phi(\Phi - \Theta)\mathbf{e}_{t-2} - \Phi^2\Theta\mathbf{e}_{t-3} \\
&= \Phi^4\tilde{\mathbf{Y}}_{t-4} + \mathbf{e}_t + (\Phi - \Theta)\mathbf{e}_{t-1} + \Phi(\Phi - \Theta)\mathbf{e}_{t-2} + \Phi^2(\Phi - \Theta)\mathbf{e}_{t-3} - \Phi^3\Theta\mathbf{e}_{t-4}.
\end{aligned}$$

From the above relations, the general form of the VARMA model with skip-sampling strategy can be obtained as $\tilde{\mathbf{Y}}_t = \Phi^{s+1}\tilde{\mathbf{Y}}_{t-s-1} + \mathbf{e}_t + \sum_{ss=1}^{s} \Phi^{ss-1}(\Phi - \Theta)\mathbf{e}_{t-ss} - \Phi^s\Theta\mathbf{e}_{t-s-1}$.

The above equation can be rewritten as:

$$\tilde{\mathbf{Y}}_t = \Phi^{s+1}\tilde{\mathbf{Y}}_{t-s-1} + \mathbf{e'}_t - \Phi^s\Theta\mathbf{e}_{t-s-1}, \tag{7}$$

where $\mathbf{e'}_t = \mathbf{e}_t + \sum_{ss=1}^{s} \Phi^{ss-1}(\Phi - \Theta)\mathbf{e}_{t-ss}$. The random noise $\mathbf{e'}_t$ is a linear combination of random noises.

Hence, when skipping s observations, $\tilde{\mathbf{Y}}_1, \tilde{\mathbf{Y}}_{s+2}, \tilde{\mathbf{Y}}_{2s+3}, \tilde{\mathbf{Y}}_{3s+4}, \ldots, \tilde{\mathbf{Y}}_{(n-1)s+n}$ fit a VARMA(1,1) model with the VAR component equal to Φ^{s+1} and the VMA component equal to $\Phi^s\Theta$. Note that, $\mathbf{e'}_t$ should be a positive linear combination of random noises (i.e. $\Phi - \Theta > \mathbf{0}$) for the observations to fit the above-mentioned VARMA model. In addition, if $s = 0$ (no skipping), the VAR and VMA components reduce to regular VARMA(1,1) parameters, i.e. Φ and Θ.

4. An adaptive max-type control chart with autocorrelation and measurement errors

We modify the control scheme proposed by Sabahno et al. [1] to include both measurement errors and autocorrelation between observations.

When the process parameters are in-control and known, the following Hotelling's T^2 statistic can be used to monitor the mean vector for each sample i:

$$T_i^2 = n(\bar{\mathbf{X}}_i\text{-}\mu_0)^T(\mathbf{\Sigma}_0)^{-1}(\bar{\mathbf{X}}_i\text{-}\mu_0), \tag{8}$$

where $T_i^2 \sim \chi^2(p)$, i.e. a chi-square distribution with p degrees of freedom.

By incorporating measurement errors (discussed in Section 2) and autocorrelation (discussed in Section 3), the Hotelling's T^2 statistic becomes:

$$T_i^2 = (\bar{\mathbf{X}}_i - \mathbf{A} - \mathbf{B}\mu_0)^T\left(\mathbf{B}\mathbf{\Sigma}_{\bar{\mathbf{Y}}_0}\mathbf{B}^{\mathbf{T}} + \frac{1}{mn}\mathbf{\Sigma}_{\boldsymbol{\varepsilon}}\right)^{-1}(\bar{\mathbf{X}}_i - \mathbf{A} - \mathbf{B}\mu_0). \tag{9}$$

Note that $\mathbf{\Sigma}_{\bar{\mathbf{Y}}_0}$ in (9) is obtained using (6).

To monitor the process variability for each sample i, we can use the following statistic:

$$W_i = \frac{(n-1)|\mathbf{S}_i|^{1/p}}{|\Sigma_0|^{1/p}}. \tag{10}$$

W_i ('exactly': when $p \leq 2$, and 'approximately': when $p > 2$) follows a gamma $\Gamma(a, b)$ distribution with parameters $a = p(n-p)/2$ and $b = 2/p(1-(p-1)(p-2)/2n)^{-1/p}$. By incorporating both measurement errors and autocorrelation, the W_i statistic becomes:

$$W_i = \frac{(n-1)|\mathbf{S}_i|^{1/p}}{\left|\mathbf{B}\boldsymbol{\Sigma}_0\mathbf{B}^{\mathbf{T}} + \frac{1}{m}\boldsymbol{\Sigma}_{\boldsymbol{\varepsilon}}\right|^{1/p}}, \tag{11}$$

where $\boldsymbol{\Sigma}_0$ in (11) is obtained using (5).

To develop the max-type scheme, we first need to transform ${T_i}^2$ and W_i statistics, as follows:

$$M_i = \Phi^{-1}[H_p(T_i^2)], \tag{12}$$

and

$$V_i = \Phi^{-1}[G_{(a,b)}(W_i)], \tag{13}$$

where $\Phi(.)$ is the standard normal cumulative distribution function, $H_p(.)$ denotes the chi-square cumulative distribution function with p degrees of freedom, and $G_{a,b}(.)$ represents the gamma cumulative distribution function with parameters a and b.

Therefore, when the process is in-control, M_i and V_i both independently follow a standard normal $N(0, 1)$ distribution.

Then, the following max-type statistic is used to represent both M_i and V_i statistics as a single statistic:

$$C_i = \max\{|M_i|, |V_i|\}\,. \tag{14}$$

This max-type statistic has a positive value. Thus, only an upper control limit UCL that can be obtained by the following equation is needed:

$$P(C_i \leq UCL) = 1 - \alpha,$$

where α is the Type-I error probability. Therefore, after simple mathematical computations, we have:

$$UCL = \Phi^{-1}\left[\frac{\sqrt{1-\alpha}+1}{2}\right]. \tag{15}$$

VP (variable parameters) adaptive scheme has been proven to be the most efficient in control charts. In such adaptive schemes, all the design (chart) parameters are allowed to vary during the online sampling. In this paper, as in most adaptive control charts so far developed, two transient states ts for each design parameter are considered ($ts \in [1, 2]$), i.e. n_1 and n_2 ($n_1 < n_2$) for sample sizes, t_1 and t_2 ($t_2 < t_1$) for sampling intervals, and, α_1 and α_2 ($\alpha_1 < \alpha_2$) for Type-I error probabilities. Consequently, we have two upper control limits: UCL_1 and UCL_2 ($UCL_2 < UCL_1$). We should also have two upper warning limits UWL_1 and UWL_2 ($UWL_1 < UCL_1$ and $UWL_2 < UCL_2$). Then, the strategy for choosing the next sample's design parameters in a VP scheme is as follows:

- When C_i is in the safe zone (i.e.$C_i \in [0, UWL]$), the design parameters for the next sample are n_1, t_1, UCL_1, UWL_1.
- When C_i is in the warning zone (i.e.$C_i \in (UWL, UCL]$), the design parameters for the next sample are n_2, t_2, UCL_2, UWL_2.
- When C_i is out of the safe zone (i.e.$C_i \in (UCL, \infty)$), the process is out-of-control and corrective actions are needed.

The following three constraints should always be satisfied in a VP control chart (each related to one design parameter):

$$ASS = n_1 P_0 + n_2(1 - P_0), \tag{16}$$

$$ASI = t_1 P_0 + t_2(1 - P_0), \tag{17}$$

$$ATE = \alpha_1 P_0 + \alpha_2(1 - P_0), \tag{18}$$

where ASS is the average sample size, ASI is the average sampling interval, ATE is the average Type-I error probability and P_0 is the probability of being in the safe state while the process is in-control, i.e.:

$$P_0 = \frac{P(C_i \le UWL)}{P(C_i \le UCL)} = \frac{P(\max\{|M_i|, |V_i|\} \le UWL)}{P(\max\{|M_i|, |V_i|\} \le UCL)} = \frac{[2\Phi(UWL) - 1]^2}{[2\Phi(UCL) - 1]^2}. \tag{19}$$

By solving Equations (16)–(18) together, we can obtain α_2 and t_1 as:

$$\alpha_2 = \frac{ATE(n_1 - n_2) - \alpha_1(ASS - n_2)}{n_1 - ASS}, \tag{20}$$

$$t_1 = \frac{ASI(n_1 - n_2) - t_2(n_1 - ASS)}{ASS - n_2}. \tag{21}$$

To obtain UWLs, we can simply solve Equation (19), as:

$$UWL_{ts} = \Phi^{-1}\left(\frac{(2\Phi(UCL_{ts}) - 1)\sqrt{P_0} + 1}{2}\right), \tag{22}$$

where $P_0 = ASS - n_2/n_1 - n_2$ is obtained by solving Equation (16).

5. Performance measures

In this paper, time-to-signal performance measures, i.e. average time to signal (ATS) and standard deviation of time to signal (SDTS), are used to evaluate the control chart's performance under different conditions. In addition, the process is assumed to be out-of-control from the beginning of the online monitoring, therefore initial (zero)-state performance measures are going to be developed in this section. To do so, we develop a Markov chain model to derive the initial-state performance measures. The Markov chain approach requires the definition of the following three states for the proposed control scheme: (i) the safe zone transient state: $C_i \in [0, UWL]$, (ii) the warning zone transient state: $C_i \in (UWL, UCL]$, and (iii) the out-of-control absorbing state: $C_i \in (UCL, \infty)$.

Then, the Markov transition probability matrix is equal to:

$$\mathbf{P} = \begin{bmatrix} p_{11} & p_{12} & p_{13} \\ p_{21} & p_{22} & p_{23} \\ p_{31} & p_{32} & p_{33} \end{bmatrix}.$$

The transient probabilities p_{11}, p_{12}, p_{21} and p_{22} for the proposed VP multivariate max-type control chart, with index *ts* representing the transient state ($ts \in [1, 2]$), are equal to:

$$\begin{aligned} p_{ts1} &= P(C_i \le UWL) = P(\max\{|M_i|, |V_i|\} \le UWL) \\ &= P(-UWL \le M_i \le UWL)P(-UWL \le V_i \le UWL), \qquad (23) \\ p_{ts2} &= P(UWL < C_i \le UCL) = P(UWL < \max\{|M_i|, |V_i|\} \le UCL) \\ &= P(-UCL \le M_i \le UCL)P(-UCL \le V_i \le UCL) \\ &\quad - P(-UWL \le M_i \le UWL)P(-UWL \le V_i \le UWL). \qquad (24) \end{aligned}$$

Equations (23) and (24) both contain the terms $P(m_1 \le M_i \le m_2)$ and $P(v_1 \le V_i \le v_2)$, where $m_1 \& v_1$ stand for *-UWL* /*-UCL* and $m_2 \& v_2$ stand for *UWL*/*UCL*. Similar to Sabahno et al. [1], we have:

$$P(m_1 \le M_i \le m_2) = P(H_p^{-1}(\Phi(m_1)) \le T_i^2 \le H_p^{-1}(\Phi(m_2))). \qquad (25)$$

We should compute Equation (25) in both in- and out-of-control conditions. When the process is in-control, $\overline{\mathbf{X}}_i \sim \text{MN}(\mathbf{A} + \mathbf{B}\mu_0, \mathbf{B}\boldsymbol{\Sigma}_{\bar{\mathbf{Y}}_0}\mathbf{B}^{\mathbf{T}} + (1/mn_{ts})\boldsymbol{\Sigma}_{\boldsymbol{\varepsilon}})$ and by letting $\mathbf{Z}_i = [\mathbf{B}\boldsymbol{\Sigma}_{\bar{\mathbf{Y}}_0}\mathbf{B}^{\mathbf{T}} + (1/mn_{ts})\boldsymbol{\Sigma}_{\boldsymbol{\varepsilon}}]^{-1/2}(\overline{\mathbf{X}}_i - \mathbf{A} - \mathbf{B}\mu_0)$, we have: $\mathbf{Z}_i \sim \text{MN}(\mathbf{0}, \mathbf{I})$. We know that: ${T_i}^2 = {\mathbf{Z}_i}^T\mathbf{Z}_i \sim \chi^2(p)$. Therefore, when the process is in-control, Equation (25) can be easily computed. When the process is out-of-control on the other hand: $\overline{\mathbf{X}}_i \sim \text{MN}(\mathbf{A} + \mathbf{B}\mu_1, \mathbf{B}\boldsymbol{\Sigma}_{\bar{\mathbf{Y}}_1}\mathbf{B}^{\mathbf{T}} + (1/mn_{ts})\boldsymbol{\Sigma}_{\boldsymbol{\varepsilon}})$ and $\mathbf{Z}_i \sim \text{MN}([\mathbf{B}\boldsymbol{\Sigma}_{\bar{\mathbf{Y}}_0}\mathbf{B}^{\mathbf{T}} + \frac{1}{mn_{ts}}\boldsymbol{\Sigma}_{\boldsymbol{\varepsilon}}]^{-1/2}\mathbf{B}(\mu_1 - \mu_0), \boldsymbol{\Lambda})$, with

$$\boldsymbol{\Lambda} = [\mathbf{B}\boldsymbol{\Sigma}_{\bar{\mathbf{Y}}_0}\mathbf{B}^{\mathbf{T}} + \frac{1}{mn_{ts}}\boldsymbol{\Sigma}_{\boldsymbol{\varepsilon}}]^{-1/2}[\mathbf{B}\boldsymbol{\Sigma}_{\bar{\mathbf{Y}}_1}\mathbf{B}^{\mathbf{T}} + \frac{1}{mn_{ts}}\boldsymbol{\Sigma}_{\boldsymbol{\varepsilon}}][\mathbf{B}\boldsymbol{\Sigma}_{\bar{\mathbf{Y}}_0}\mathbf{B}^{\mathbf{T}} + \frac{1}{mn_{ts}}\boldsymbol{\Sigma}_{\boldsymbol{\varepsilon}}]^{-1/2}.$$

Consequently, we have ${\mathbf{Z}_i}^T\boldsymbol{\Lambda}^{-1}\mathbf{Z}_i \sim \chi^2(p, \lambda)$, i.e. a non-central chi-square distribution with the non-centrality parameter:

$$\begin{aligned} \lambda = [\mathbf{B}(\mu_1 - \mu_0)]^T &[\mathbf{B}\boldsymbol{\Sigma}_{\bar{\mathbf{Y}}_0}\mathbf{B}^{\mathbf{T}} + \frac{1}{mn_{ts}}\boldsymbol{\Sigma}_{\boldsymbol{\varepsilon}}]^{-1/2}\boldsymbol{\Lambda}^{-1/2}\boldsymbol{\Lambda}^{-1/2}[\mathbf{B}\boldsymbol{\Sigma}_{\bar{\mathbf{Y}}_0}\mathbf{B}^{\mathbf{T}} + \frac{1}{mn_{ts}}\boldsymbol{\Sigma}_{\boldsymbol{\varepsilon}}]^{-1/2} \\ &\mathbf{B}(\mu_1 - \mu_0). \end{aligned}$$

By replacing $\boldsymbol{\Lambda}$ with its formula, the non-centrality parameter is computed as:

$$\lambda = [\mathbf{B}(\mu_1 - \mu_0)]^T\left(\mathbf{B}\boldsymbol{\Sigma}_{\bar{\mathbf{Y}}_1}\mathbf{B}^{\mathbf{T}} + \frac{1}{mn_{ts}}\boldsymbol{\Sigma}_{\boldsymbol{\varepsilon}}\right)^{-1}\mathbf{B}(\mu_1 - \mu_0). \qquad (26)$$

Since it is not possible to obtain the distribution of ${T_i}^2 = {\mathbf{Z}_i}^T\mathbf{Z}_i$ for an out-of-control condition (we could only find the distribution of ${\mathbf{Z}_i}^T\boldsymbol{\Lambda}^{-1}\mathbf{Z}_i$, not ${\mathbf{Z}_i}^T\mathbf{Z}_i$), we cannot directly compute Equation (25) in the case of an out-of-control condition. Hence, similar to Sabahno et al. [1], it will be assumed that $[\mathbf{B}\boldsymbol{\Sigma}_{\bar{\mathbf{Y}}_1}\mathbf{B}^{\mathbf{T}} + (1/mn_{ts})\boldsymbol{\Sigma}_{\boldsymbol{\varepsilon}}] =$

$\tau_1[\mathbf{B}\boldsymbol{\Sigma}_{\bar{\mathbf{Y}}_0}\mathbf{B}^{\mathbf{T}}+(1/mn_{ts})\boldsymbol{\Sigma}_{\boldsymbol{\varepsilon}}]$, with $\tau_1 > 0$. Therefore, we have $\boldsymbol{\Lambda}^{-1} = (1/\tau_1)\mathbf{I}$ and, consequently, $(1/\tau_1)T_i^2 = (1/\tau_1)\mathbf{Z}_i{}^T\mathbf{Z}_i \sim \chi^2(p,\lambda)$ with

$$\lambda = \frac{1}{\tau_1}(\mu_1 - \mu_0)^T\mathbf{B}^{\mathbf{T}}\left(\mathbf{B}\boldsymbol{\Sigma}_{\bar{\mathbf{Y}}_0}\mathbf{B}^{\mathbf{T}}+\frac{1}{mn_{ts}}\boldsymbol{\Sigma}_{\boldsymbol{\varepsilon}}\right)^{-1}\mathbf{B}(\mu_1 - \mu_0\,).$$

Now, we can compute Equation (25) in an out-of-control condition as:

$$P(m_1 \le M_i \le m_2) = [H_{p,\lambda}(H_p^{-1}(\Phi(m_2)) \times (1/\tau_1)) - H_{p,\lambda}(H_p^{-1}(\Phi(m_1)) \times (1/\tau_1))]. \tag{27}$$

To compute $P(\nu_1 \le V_i \le \nu_2)$, by adopting a similar approach, we have:

$$P(\nu_1 \le V_i \le \nu_2) = P(G_{(a,b)}^{-1}(\Phi(\nu_1)) \le W_i \le G_{(a,b)}^{-1}(\Phi(\nu_2)))\,. \tag{28}$$

When the process is out-of-control, the distribution of W_i is obtained by multiplying $|\mathbf{B}\boldsymbol{\Sigma}_0\mathbf{B}^{\mathbf{T}}+(1/m)\boldsymbol{\Sigma}_{\boldsymbol{\varepsilon}}|$ by $|\mathbf{B}\boldsymbol{\Sigma}_1\mathbf{B}^{\mathbf{T}}+(1/m)\boldsymbol{\Sigma}_{\boldsymbol{\varepsilon}}|/|\mathbf{B}\boldsymbol{\Sigma}_1\mathbf{B}^{\mathbf{T}}+(1/m)\boldsymbol{\Sigma}_{\boldsymbol{\varepsilon}}| = 1$ in Equation (28), as follows:

$$\begin{aligned} P(G_{(a,b)}^{-1}(\Phi(\nu_1)) &\le \frac{(n_s-1)|S_i|^{1/p}}{[|\mathbf{B}\boldsymbol{\Sigma}_0\mathbf{B}^{\mathbf{T}}+(1/m)\boldsymbol{\Sigma}_{\boldsymbol{\varepsilon}}||\mathbf{B}\boldsymbol{\Sigma}_1\mathbf{B}^{\mathbf{T}}+(1/m)\boldsymbol{\Sigma}_{\boldsymbol{\varepsilon}}|/|\mathbf{B}\boldsymbol{\Sigma}_1\mathbf{B}^{\mathbf{T}}+(1/m)\boldsymbol{\Sigma}_{\boldsymbol{\varepsilon}}|]^{1/p}} \\ &\le G_{(a,b)}^{-1}(\Phi(\nu_2))). \end{aligned}$$

Then, assuming $\tau_2 = [|\mathbf{B}\boldsymbol{\Sigma}_1\mathbf{B}^{\mathbf{T}}+(1/m)\boldsymbol{\Sigma}_{\boldsymbol{\varepsilon}}/\mathbf{B}\boldsymbol{\Sigma}_0\mathbf{B}^{\mathbf{T}}+(1/m)\boldsymbol{\Sigma}_{\boldsymbol{\varepsilon}}|]^{1/p}$, we have:

$$P(\nu_1 \le V_i \le \nu_2) = [G_{(a,b)}(G_{(a,b)}^{-1}(\Phi(\nu_2)) \times (1/\tau_2)) - G_{(a,b)}(G_{(a,b)}^{-1}(\Phi(\nu_1)) \times (1/\tau_2))]. \tag{29}$$

Equations (23) and (24) can be computed using $P(m_1 \le M_i \le m_2)$ and $P(\nu_1 \le V_i \le \nu_2)$, by replacing m_1&ν_1 with *-UWL/-UCL* and m_2&ν_2 with *UWL/UCL* in Equations (27) and (29).

Although τ_2 has a deterministic value, τ_1 on the other hand, does not have a deterministic value and it should be estimated. To estimate τ_1, we can use the generalization of matrices in order to change them into numbers. The generalized form of a variance-covariance matrix (it's determinant) is called the generalized variance. Hence, following the same approach as Sabahno et al. [1], the value of τ_1 can be estimated by $|\boldsymbol{\Lambda}|^{1/p}$, i.e.

$$\tau_1 \approx \left[\frac{\left|\mathbf{B}\boldsymbol{\Sigma}_{\bar{\mathbf{Y}}_1}\mathbf{B}^{\mathbf{T}}+\frac{1}{mn_{ts}}\boldsymbol{\Sigma}_{\boldsymbol{\varepsilon}}\right|}{\left|\mathbf{B}\boldsymbol{\Sigma}_{\bar{\mathbf{Y}}_0}\mathbf{B}^{\mathbf{T}}+\frac{1}{mn_{ts}}\boldsymbol{\Sigma}_{\boldsymbol{\varepsilon}}\right|}\right]^{1/p}.$$

More specifically, τ_1 is estimated such that the relationship $[\mathbf{B}\boldsymbol{\Sigma}_{\bar{\mathbf{Y}}_1}\mathbf{B}^{\mathbf{T}}+(1/mn_{ts})\boldsymbol{\Sigma}_{\boldsymbol{\varepsilon}}] = \tau_1[\mathbf{B}\boldsymbol{\Sigma}_{\bar{\mathbf{Y}}_0}\mathbf{B}^{\mathbf{T}}+(1/mn_{ts})\boldsymbol{\Sigma}_{\boldsymbol{\varepsilon}}]$ is approximately held.

Note that, in the case of no autocorrelation and/or no measurement errors: $\tau_1 = \tau_2$.

To obtain the other transition probabilities, we have $p_{13} = 1 - p_{11} - p_{12}$, $p_{23} = 1 - p_{21} - p_{22}$, $p_{31} = p_{32} = 0$ and $p_{33} = 1$. Now, we can compute our performance measures

using the following equations:

$$\text{ATS} = \mathbf{b}'(\mathbf{I} - Q)^{-1}\mathbf{t}, \tag{30}$$

$$\text{SDTS} = \sqrt{\mathbf{b}'(\mathbf{I} - \mathbf{Q})^{-1}(2\mathbf{D_t}(\mathbf{I} - \mathbf{Q})^{-1}\mathbf{t} - \mathbf{t}^{(2)}) - (\text{ATS})^2}, \tag{31}$$

where $\mathbf{b}' = (b_1, b_2)$ is the vector of starting probabilities such that $b_1 + b_2 = 1$, $\mathbf{I}$ is the identity matrix of order 2, $\mathbf{Q}$ is a 2×2 transition probability matrix for the transient states, $\mathbf{t} = (t_1, t_2)'$ is the vector of sampling intervals, $\mathbf{D_t}$ is the 2×2 diagonal matrix with the diagonal elements of $\mathbf{t}$, $\mathbf{t}^{(2)}$ contains the squares of the elements of the vector $\mathbf{t}$.

In the beginning, when the process is assumed to be in-control ($\mu_1 = \mu_0 \& \mathbf{\Sigma}_{e_1} = \mathbf{\Sigma}_{e_0}$), b_1 and b_2 are obtained as follows:

$$b_1 = \frac{p_{11}}{p_{11} + p_{12}},$$
$$b_2 = \frac{p_{22}}{p_{21} + p_{22}}.$$

6. Numerical analyses

In this section, the effects of autocorrelation and measurement errors on the proposed control chart as well as some solutions to alleviate their negative effects will be investigated. To better and easier analyse these effects, we only consider autocorrelational effects and neglect the cross-correlational effects, i.e. Φ and Θ matrices are assumed to be diagonal. In addition, although Φ and Θ can take any value in $(-1, 1)$, since positive autocorrelations are most common in real practice, following Costa and Castagliola [34], we only consider positive autocorrelations in this paper.

6.1. The effects of measurement errors and autocorrelation

For the case of $p = 2$, we have $\Phi = \begin{bmatrix} \phi_{1,1} & 0 \\ 0 & \phi_{2,2} \end{bmatrix}$ and $\Theta = \begin{bmatrix} \theta_{1,1} & 0 \\ 0 & \theta_{2,2} \end{bmatrix}$, and we assume the following values for the diagonal elements:

$$\theta = (\theta_{1,1}, \theta_{2,2}) \in \{(0,0), (0.4, 0.3), (0.7, 0.8)\} \textit{ and}$$
$$\phi = (\phi_{1,1}, \phi_{2,2}) \in \{(0,0), (0.2, 0.3), (0.6, 0.5)\}.$$

For the in-control random noise variance-covariance matrix, we assume that $\mathbf{\Sigma}_{e_0} = \begin{bmatrix} 1 & 0.5 \\ 0.5 & 1 \end{bmatrix}$. Then, when shifted, we assume that $\mathbf{\Sigma}_{e_1} = \tau \mathbf{\Sigma}_{e_0}$. Note that, in the case of no autocorrelation ($\Phi \& \Theta = 0$), the random noise variance-covariance matrix is the same as the quality characteristics' variance-covariance matrix (i.e. $\mathbf{\Sigma}_0 = \mathbf{\Sigma}_{e_0}$ and $\mathbf{\Sigma}_1 = \mathbf{\Sigma}_{e_1}$).

In this paper, we assume that the level of autocorrelation, as well as measurement errors, do not change throughout the process monitoring, and shifts only occur for the mean vector and also for the random noise variance-covariance matrix. For the mean vector shifts, we assume: $\mu_0 = (1, 1) \rightarrow \mu_1 \in \{(1, 1), (1.1, 1.1), (1.5, 1.5)\}$ and for the random noise variance-covariance matrix shifts we assume: $\tau \in \{1.02, 1.2, 1.5\}$.

We also assume that $ATE = 0.005$, $ASI = 1$, $ASS = 10$, $(n_1, n_2) = (5, 15)$, $t_2 = 0.1$, $\mu_0 = (0, 0)$ and $\alpha_1 = 0.004$. In addition, for the measurement errors model parameters, we assume: $\mathbf{\Sigma}_\varepsilon = \begin{bmatrix} \varepsilon_1 & 0 \\ 0 & \varepsilon_2 \end{bmatrix}$, so that $\varepsilon = (\varepsilon_1, \varepsilon_2) \in \{(0, 0), (0.5, 0.5), (1, 1)\}$, $\mathbf{B} = \mathbf{I}$ and $m = 1$. The results for the $p = 2$ case for different mean vector shifts are shown in Tables 1–3.

As can be seen in Tables 1–3, for any autocorrelation level (different Φ and Θ values) we have:

- As the shift in the random noise variance-covariance matrix (τ) increases, the chart signals faster.
- As the mean shift ($\mu_1 - \mu_0$) increases, the chart signals faster.
- As the measurement errors (ε) increase, the control chart signals slower.
- In all cases, the ATS and SDTS values are very close, but the SDTS values are always slightly larger.

In addition, in Table 1 (zero mean shift), when there are no measurement errors ($\varepsilon = \mathbf{0}$), and for any shift size in the random noise variance-covariance matrix (any τ value), different values of Φ and Θ have no effect on the chart's performance. However, when the mean shift is not zero (Tables 2 and 3), when the value of Φ (AR component) is larger, the chart signals slower and when the Θ value (MA component) is larger, the chart signals faster. Having said that, when measurement errors are available in the process ($\varepsilon > \mathbf{0}$), the above-mentioned rule is not always valid.

We repeat the previous analysis by increasing p to 4 (four quality characteristics) and by keeping the previous value assumptions for the design and process parameters. Tables 4–6 contain the information regarding the $p = 4$ case; with three different mean vector shift sizes. All of the previous conclusions for the $p = 2$ case are valid for the $p = 4$ case as well. However, all of the ATS/SDTS values are smaller when $p = 4$ (the chart signals faster when there are more quality characteristics).

6.2. Reducing the autocorrelation effect

In this section, assuming there are no measurement errors in the process, we try to apply the developed skip-sampling strategy to investigate its effect on the chart's performance. In this section as well as the next section, we only consider the case of $p = 3$. The design and process parameters are assumed to be as before, except for θ which is fixed to $\theta = (0.1, 0.1, 0.1)$ and ϕ changes from $(0.2, 0.2, 0.2)$ to $(0.4, 0.4, 0.4)$, $(0.6, 0.6, 0.6)$ and $(0.8, 0.8, 0.8)$ in each plot. We have three plots in Figure 1, each having a different mean vector shift size of $\mu_1 \in \{(1.1, 1.1, 1.1), (1.5, 1.5, 1.5), (2, 2, 2)\}$. τ is assumed to be 1.2 in this analysis to represent the random noise variance-covariance matrix shift. We assume that the number of skipped samples (s) will vary from 0 to 20 in each plot and we will only use the ATS as the performance measure here.

As can be seen in Figure 1, as the number of skipped samples increases, the chart performs better (signals faster), and the negative effect of autocorrelation decreases. However, skipping samples is only effective until some s value, and after that, the chart becomes insensitive to the change in the value of s. The larger the value of Φ is,

Table 1. ATS, SDTS with $p = 2$ and the mean vector $\mu_1 = (1, 1)$.

		ϕ								
		(0,0)			(0.2,0.3)			(0.6,0.5)		
		θ			θ			θ		
		(0,0)	(0.4,0.3)	(0.7,0.8)	(0,0)	(0.4,0.3)	(0.7,0.8)	(0,0)	(0.4,0.3)	(0.7,0.8)
		$\tau = 1.02$								
	(0,0)	184.7007, 184.7858	184.7007, 184.7858	184.7007, 184.7858	184.7007, 184.7858	184.7007, 184.7858	184.7007, 184.7858	184.7007, 184.7858	184.7007, 184.7858	184.7007, 184.7858
ε	(0.5,0.5)	190.7369, 190.8211	191.4853, 191.5693	191.8912, 191.9742	189.9320, 190.0162	191.0031, 191.0871	192.0361, 192.1190	188.5068, 188.5911	189.8558, 189.9401	191.5369, 191.6201
	(1,1)	193.1862, 193.2702	193.8968, 193.9807	194.0306, 194.1138	192.2859, 192.3700	193.4543, 193.5383	194.2854, 194.3686	190.5229, 190.6071	192.1872, 192.2715	193.9428, 194.0261
		$\tau = 1.2$								
	(0,0)	52.6587, 52.8741	52.6587, 52.8741	52.6587, 52.8741	52.6587, 52.8741	52.6587, 52.8741	52.6587, 52.8741	52.6587, 52.8741	52.6587, 52.8741	52.6587, 52.8741
ε	(0.5,0.5)	95.4640, 95.6253	97.0104, 97.1814	92.9631, 93.1482	90.6272, 90.7878	96.2832, 96.4469	97.2656, 97.4390	80.5459, 80.7144	90.4398, 90.6008	98.0415, 98.2040
	(1,1)	120.3320, 120.4645	122.4973, 122.6384	116.1205, 116.2782	113.5910, 113.7240	121.5591, 121.6934	122.1623, 122.3065	98.9846, 99.1275	113.1486, 113.2826	123.7106, 123.8434
		$\tau = 1.5$								
	(0,0)	6.4337, 6.6056	6.4337, 6.6056	6.4337, 6.6056	6.4337, 6.6056	6.4337, 6.6056	6.4337, 6.6056	6.4337, 6.6056	6.4337, 6.6056	6.4337, 6.6056
ε	(0.5,0.5)	21.9733, 22.2092	21.6188, 21.8760	18.2720, 18.5433	19.8722, 20.0951	22.0436, 22.2862	20.8229, 21.0886	15.3682, 15.5769	19.8854, 20.1077	22.3142, 22.5629
	(1,1)	40.8550, 41.0833	40.2883, 40.5435	32.2276, 32.5099	35.9791, 36.1958	41.1998, 41.4360	38.1294, 38.3971	25.7767, 25.9857	35.8564, 36.0729	41.7571, 42.0001

Table 2. ATS, SDTS with $p = 2$ and the mean vector $\mu_1 = (1.1, 1.1)$.

		ϕ								
		(0,0)			(0.2,0.3)			(0.6,0.5)		
		θ			θ			θ		
		(0,0)	(0.4,0.3)	(0.7,0.8)	(0,0)	(0.4,0.3)	(0.7,0.8)	(0,0)	(0.4,0.3)	(0.7,0.8)
		$\tau = 1.02$								
	(0,0)	162.3570, 162.4846	138.7565, 138.9450	78.1241, 78.5223	171.2617, 171.3704	154.6227, 154.7697	97.1568, 97.4907	179.1806, 179.2737	172.7280, 172.8324	129.4982, 129.7291
ε	(0.5,0.5)	173.5566, 173.6725	163.7274, 163.8681	149.3881, 149.5717	178.5266, 178.6306	170.3386, 170.4625	153.0619, 153.2359	183.3363, 183.4282	179.4494, 179.5506	162.5063, 162.6539
	(1,1)	179.3291, 179.4385	174.0048, 174.1277	167.7332, 167.8731	182.4445, 182.5457	177.5443, 177.6582	169.3387, 169.4754	185.6978, 185.7891	183.0763, 83.1755	173.5982, 173.7237
		$\tau = 1.2$								
	(0,0)	47.5871, 47.8105	42.2870, 42.5274	28.0424, 28.3599	49.5963, 49.8154	45.8474, 46.0761	32.7156, 33.0091	51.3986, 51.6146	49.9330, 50.1506	40.1911, 40.4496
ε	(0.5,0.5)	87.2470, 87.4253	84.6464, 84.8450	77.0092, 77.2353	85.2759, 85.4470	86.5846, 86.7692	81.2388, 81.4536	78.3772, 78.5488	85.5224, 85.6920	84.9560, 85.1516
	(1,1)	111.5965, 111.7471	110.8632, 111.0290	103.3102, 103.4969	107.4771, 107.6224	111.7162, 111.8713	108.7416, 108.9165	96.3055, 96.4529	107.4442, 107.5891	111.6499, 111.8104
		$\tau = 1.5$								
	(0,0)	6.1621, 6.3277	5.8672, 6.0287	4.9833, 5.1444	6.2708, 6.4386	6.0666, 6.2308	5.2937, 5.4551	6.3672, 6.5372	34.5046, 34.7218	5.7466, 5.9102
ε	(0.5,0.5)	20.7850, 21.0187	19.9834, 20.2365	16.6255, 16.8899	19.1416, 19.3627	20.6690, 20.9090	18.9199, 19.1809	15.1282, 15.3354	19.2103, 19.4305	20.5310, 20.7776
	(1,1)	38.6571, 38.8876	37.6970, 37.9535	30.1978, 30.4782	34.5406, 34.7585	38.7861, 39.0245	35.5513, 35.8194	25.2960, 25.5044	34.5046, 34.7218	38.9680, 39.2138

Table 3. ATS, SDTS with $p = 2$ and the mean vector $\mu_1 = (1.5, 1.5)$.

		ϕ								
		(0,0)			(0.2,0.3)			(0.6,0.5)		
		θ			θ			θ		
		(0,0)	(0.4,0.3)	(0.7,0.8)	(0,0)	(0.4,0.3)	(0.7,0.8)	(0,0)	(0.4,0.3)	(0.7,0.8)
					$\tau = 1.02$					
	(0,0)	7.0808, 7.3810	1.8541, 2.0367	1.3127, 1.4539	21.2162, 21.5769	3.6505, 3.8941	1.3745, 1.5524	75.9497, 76.2166	22.0751, 22.4250	1.7690, 2.0001
ε	(0.5,0.5)	13.5368, 13.8988	4.5060, 4.7854	2.0877, 2.3270	30.3290, 30.7012	8.8991, 9.2380	2.3568, 2.6073	83.4942, 83.7560	33.0379, 33.3967	4.0395, 4.3390
	(1,1)	21.5256, 21.9126	9.7796, 10.1378	4.9969, 5.3162	39.4200, 39.7906	16.1585, 16.5417	5.6740, 6.0073	89.9374, 90.1933	43.0456, 43.4006	8.9748, 9.3485
					$\tau = 1.2$					
	(0,0)	4.8148, 5.0090	1.7455, 1.8811	1.2839, 1.4005	10.8631, 11.1011	2.9446, 3.1097	1.3366, 1.4804	27.4325, 27.6619	12.8468, 13.0764	1.5797, 1.7642
ε	(0.5,0.5)	9.8262, 10.1086	3.9230, 4.1482	1.9879, 2.1887	18.6239, 18.9134	6.9538, 7.2204	2.2247, 2.4344	39.4379, 39.6711	21.2305, 21.5067	3.5764, 3.8190
	(1,1)	16.2638, 16.5889	8.3158, 8.6213	4.5372, 4.8091	26.3670, 26.6768	12.7872, 13.1104	5.1290, 5.4152	48.5411, 48.7758	29.1702, 29.4657	7.8552, 8.1733
					$\tau = 1.5$					
	(0,0)	2.4021, 2.4728	1.5039, 1.5707	1.2294, 1.2995	3.3827, 3.4757	1.9388, 2.0059	1.2678, 1.3532	4.9274, 5.0550	3.6216, 3.7148	1.4255, 1.5283
ε	(0.5,0.5)	5.2554, 5.4211	2.8596, 2.9947	1.7584, 1.8927	7.5770, 7.7532	4.1986, 4.3543	1.9248, 2.0641	10.2763, 10.4513	8.2148, 8.3881	2.7017, 2.8513
	(1,1)	9.4188, 9.6494	5.7499, 5.9643	3.4884, 3.6720	12.6128, 12.8357	7.9343, 8.1623	3.9471, 4.1465	16.0243, 16.2203	13.5064, 13.7238	5.5524, 5.7754

Table 4. ATS, SDTS with $p = 4$ and the mean vector $\mu_1 = (1, 1, 1, 1)$.

		ϕ								
		(0,0,0,0)			(0.2,0.3,0.2,0.3)			(0.6,0.5,0.6,0.5)		
		θ			θ			θ		
		(0,0, 0,0)	(0.4,0.3, 0.4,0,3)	(0.7,0.8, 0.7,0.8)	(0,0, 0,0)	(0.4,0.3, 0.4,0,3)	(0.7,0.8, 0.7,0.8)	(0,0, 0,0)	(0.4,0.3, 0.4,0,3)	(0.7,0.8, 0.7,0.8)
					$\tau = 1.02$					
	(0,0, 0,0)	168.8696, 168.9827	168.8696, 168.9827	168.8696, 168.9827	168.8696, 168.9827	168.8696, 168.9827	168.8696, 168.9827	168.8696, 168.9827	168.8696, 168.9827	168.8696, 168.9827
ε	(0.5,0.5, 0.5,0.5)	183.8628, 183.9567	184.1530, 184.2477	183.1771, 183.2736	182.7301, 182.8245	184.0169, 184.1110	184.1829, 184.2776	180.0161, 180.1129	182.6956, 182.7901	184.3641, 184.4577
	(1,1, 1,1)	188.7798, 188.8691	189.0694, 189.1593	187.9820, 188.0735	187.6409, 187.7306	188.9435, 189.0329	189.0106, 189.1005	184.7459, 184.8376	187.5790, 187.6689	189.2543, 189.3434
					$\tau = 1.2$					
	(0,0, 0,0)	5.2714, 5.5946	5.2714, 5.5946	5.2714, 5.5946	5.2714, 5.5946	5.2714, 5.5946	5.2714, 5.5946	5.2714, 5.5946	5.2714, 5.5946	5.2714, 5.5946
ε	(0.5,0.5, 0.5,0.5)	26.1616, 26.5603	24.0329, 24.4476	18.2753, 18.7010	23.9724, 24.3638	25.6680, 26.0719	21.9106, 22.3328	17.8337, 18.2173	24.1902, 24.5804	25.0222, 25.4320
	(1,1, 1,1)	52.1952, 52.5512	48.2121, 48.5928	35.7083, 36.1250	47.5795, 47.9340	51.4109, 51.7739	43.7487, 44.1456	34.3316, 34.6993	47.9076, 48.2603	48.2603, 50.5963
					$\tau = 1.5$					
	(0,0, 0,0)	1.3670, 1.5226	1.3670, 1.5226	1.3670, 1.5226	1.3670, 1.5226	1.3670, 1.5226	1.3670, 1.5226	1.3670, 1.5226	1.3670, 1.5226	1.3670, 1.5226
ε	(0.5,0.5, 0.5,0.5)	2.1636, 2.4074	2.0645, 2.3225	1.8277, 2.0884	2.0461, 2.2751	2.1396, 2.3884	1.9714, 2.2342	1.7692, 1.9781	2.0571, 2.2852	2.1081, 2.3630
	(1,1, 1,1)	4.4670, 4.7751	3.9126, 4.2300	2.7605, 3.0630	3.9396, 4.2221	4.3352, 4.6478	3.4261, 3.7414	2.6938, 2.9296	3.9909, 4.2727	4.1456, 4.4629

Table 5. ATS, SDTS with $p = 4$ and the mean vector $\mu_1 = (1.1, 1.1, 1.1, 1.1)$.

		ϕ								
		(0,0,0,0)			(0.2,0.3,0.2,0.3)			(0.6,0.5,0.6,0.5)		
		θ			θ			θ		
		(0,0, 0,0)	(0.4,0.3, 0.4,0,3)	(0.7,0.8, 0.7,0.8)	(0,0, 0,0)	(0.4,0.3, 0.4,0,3)	(0.7,0.8, 0.7,0.8)	(0,0, 0,0)	(0.4,0.3, 0.4,0,3)	(0.7,0.8, 0.7,0.8)
					$\tau = 1.02$					
	(0,0, 0,0)	155.0573, 155.1967	138.5053, 138.6888	87.0600, 87.4267	160.6864, 160.8137	149.3488, 149.5030	104.8572, 105.1611	165.5413, 165.6591	161.6533, 161.7778	129.5698, 129.7924
ε	(0.5,0.5, 0.5,0.5)	171.3917, 171.5092	161.9238, 162.0661	143.4616, 143.6613	174.8297, 174.9380	168.3650, 168.4902	149.0166, 149.2007	176.6056, 176.7074	175.5685, 175.6745	160.2935, 160.4440
	(1,1, 1,1)	177.9054, 178.0150	171.7398, 171.8653	162.0059, 162.1588	180.3769, 180.4793	175.9372, 176.0519	164.9652, 165.1113	181.4230, 181.5196	180.9405, 181.0412	171.1371, 171.2663
					$\tau = 1.2$					
	(0,0, 0,0)	5.1456, 5.4600	5.0004, 5.3072	4.5139, 4.8077	5.1960, 5.5136	5.0953, 5.4071	4.6980, 4.9967	5.2403, 5.5610	5.2046, 5.5227	4.9254, 5.2320
ε	(0.5,0.5, 0.5,0.5)	25.1923, 25.5848	22.6624, 23.0675	16.7789, 17.1910	23.3900, 23.7769	24.5277, 24.9243	20.1679, 20.5789	17.6552, 18.0362	23.6513, 24.0371	23.4564, 23.8581
	(1,1, 1,1)	50.0970, 50.4514	45.5835, 45.9616	33.4287, 33.8400	46.2391, 46.5919	49.0580, 49.4193	40.8572, 41.2512	33.9023, 34.2682	46.6481, 46.9989	47.3086, 47.6792
					$\tau = 1.5$					
	(0,0, 0,0)	1.3630, 1.5156	1.3597, 1.5100	1.3548, 1.5025	1.3645, 1.5181	1.3618, 1.5136	1.3567, 1.5054	1.3658, 1.5205	1.3646, 1.5183	1.3599, 1.5106
ε	(0.5,0.5, 0.5,0.5)	2.1450, 2.3841	2.0396, 2.2905	1.8044, 2.0569	2.0352, 2.2613	2.1182, 2.3614	1.9430, 2.1976	1.7660, 1.9736	2.0469, 2.2721	2.0805, 2.3285
	(1,1, 1,1)	4.3983, 4.7004	3.8384, 4.1477	2.7139, 3.0081	3.8989, 4.1773	4.2611, 4.5668	3.3562, 3.6625	2.6840, 2.9180	3.9520, 4.2299	4.0604, 4.3697

Table 6. ATS, SDTS with $p = 4$ and the mean vector $\mu_1 = (1.5, 1.5, 1.5, 1.5)$.

		ϕ								
		(0,0,0,0)			(0.2,0.3,0.2,0.3)			(0.6,0.5,0.6,0.5)		
		θ			θ			θ		
		(0,0, 0,0)	(0.4,0.3, 0.4,0,3)	(0.7,0.8, 0.7,0.8)	(0,0, 0,0)	(0.4,0.3, 0.4,0,3)	(0.7,0.8, 0.7,0.8)	(0,0, 0,0)	(0.4,0.3, 0.4,0,3)	(0.7,0.8, 0.7,0.8)
					$\tau = 1.02$					
	(0,0, 0,0)	8.3789, 8.7204	1.9158, 2.1311	1.3412, 1.5072	25.6655, 26.0508	3.8417, 4.1203	1.4068, 1.6141	84.6742, 84.9376	32.5799, 32.9416	1.6567, 1.9342
ε	(0.5,0.5, 0.5,0.5)	13.3207, 13.7081	3.4849, 3.7664	1.6723, 1.9307	33.5916, 33.9840	7.7677, 8.1234	1.8319, 2.1011	93.2275, 93.4821	40.4797, 40.8465	2.9924, 3.2980
	(1,1, 1,1)	19.0885, 19.4981	6.3593, 6.7084	2.6508, 2.9445	40.9201, 41.3100	12.7104, 13.1086	3.0762, 3.3849	99.2327, 99.4808	47.6412, 48.0056	5.6639, 6.0294
					$\tau = 1.2$					
	(0,0, 0,0)	2.4315, 2.5794	1.5252, 1.6478	1.2630, 1.3640	3.3198, 3.5150	1.9318, 2.0649	1.3075, 1.4347	4.4441, 4.7046	3.5244, 3.7256	1.4509, 1.6191
ε	(0.5,0.5, 0.5,0.5)	6.0251, 6.2744	2.5375, 2.7221	1.5478, 1.7448	9.8912, 10.1791	4.2723, 4.4949	1.6607, 1.8642	13.1468, 13.4685	10.9985, 11.2874	2.3190, 2.5278
	(1,1, 1,1)	10.5640, 10.8766	4.5573, 4.8142	2.2574, 2.4809	17.1161, 17.4411	7.7923, 8.0891	2.5796, 2.8153	23.4159, 23.7436	18.9783, 19.2975	4.2007, 4.4713
					$\tau = 1.5$					
	(0,0, 0,0)	1.2751, 1.3645	1.2143, 1.2641	1.1567, 1.1711	1.3064, 1.4176	1.2518, 1.3260	1.1754, 1.2041	1.3381, 1.4720	1.3098, 1.4230	1.2189, 1.2774
ε	(0.5,0.5, 0.5,0.5)	1.7204, 1.8682	1.5021, 1.6325	1.3394, 1.4617	1.7820, 1.9447	1.6363, 1.7771	1.3833, 1.5158	1.6889, 1.8671	1.8085, 1.9720	1.5010, 1.6428
	(1,1, 1,1)	2.7401, 2.9169	2.0545, 2.2108	1.5916, 1.7531	2.9174, 3.1077	2.4770, 2.6448	1.7107, 1.8743	2.4497, 2.6449	3.0194, 3.2117	2.0499, 2.2143

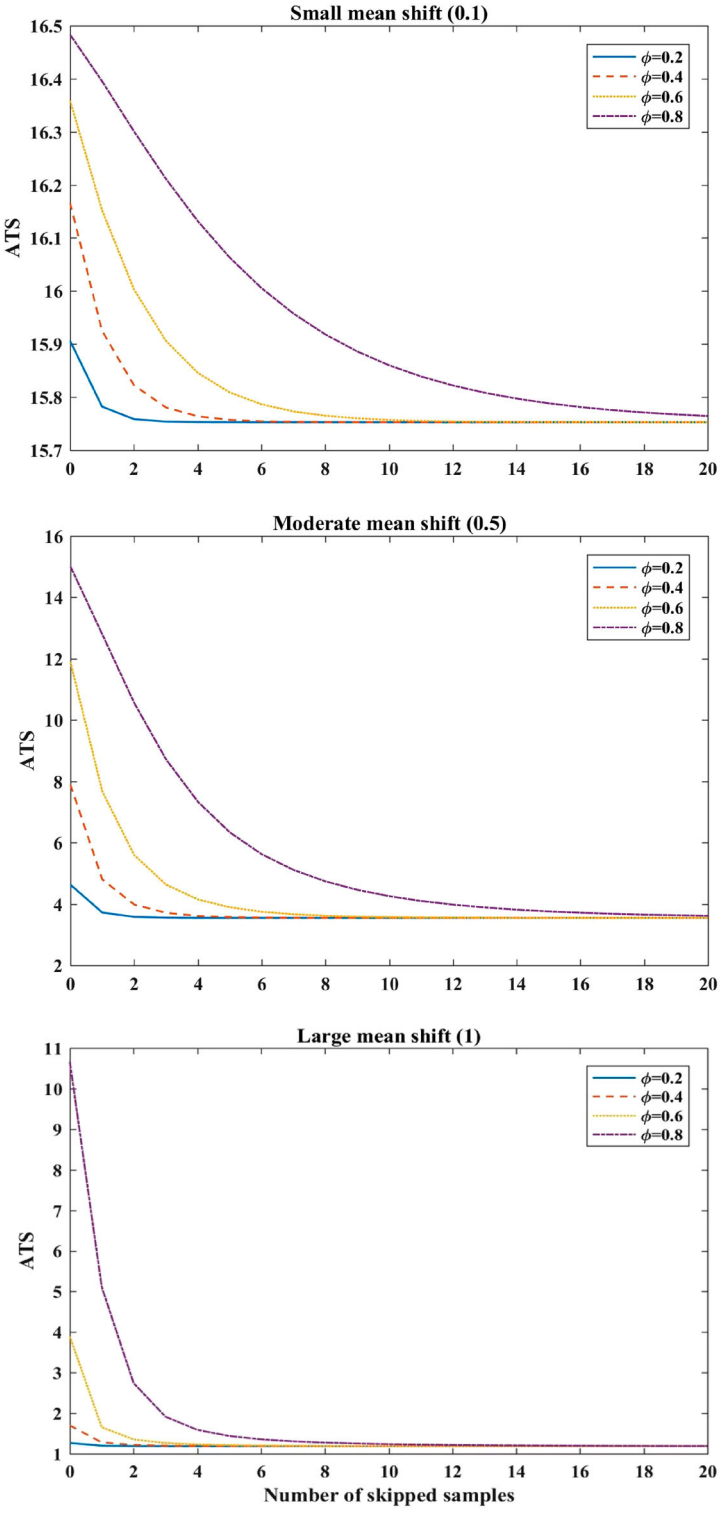

Figure 1. ATS versus Number of skipped samples (s) for small, moderate, and large (respectively, from top to bottom) mean vector shifts for $p = 3$.

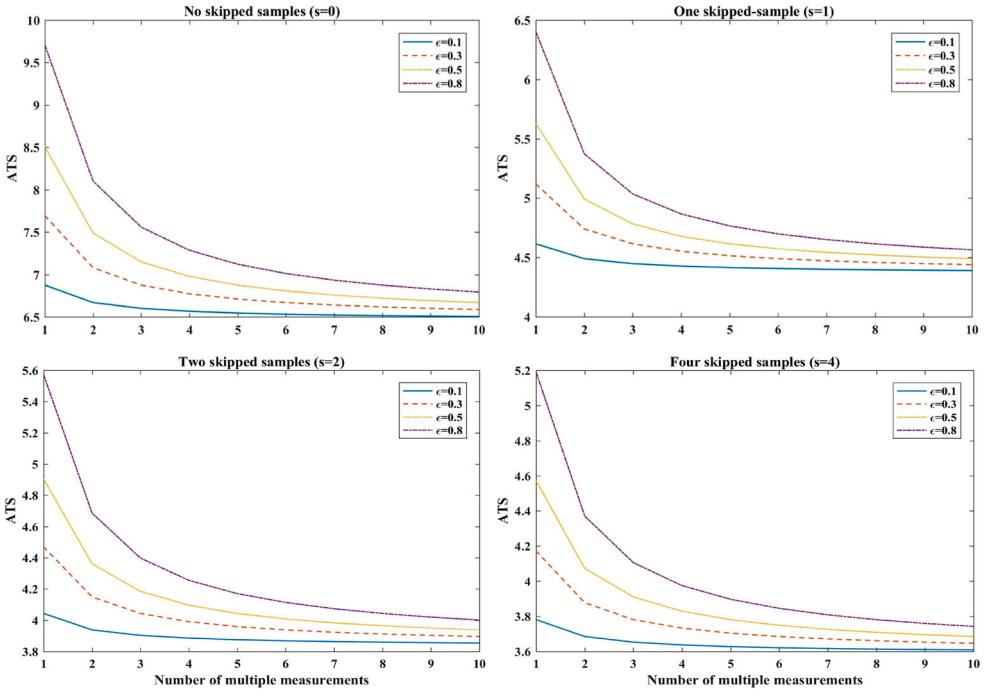

Figure 2. ATS versus Number of multiple measurements (m) with zero, small, moderate, and large numbers of skipped samples for $p = 3$.

the more skipped samples are needed until the chart becomes insensitive to the number of skipped samples. On the contrary, as the mean vector shift increases, the chart needs fewer skipped samples before it becomes insensitive to the number of skipped samples.

6.3. Reducing the measurement errors effect

Sabahno et al. [4] showed that multiple measurements (m) will alleviate the effect of measurement errors in the case of no autocorrelation in the process. In this section, we will investigate the effect of multiple measurements when there is also autocorrelation in the process and in the case the skipped-sampling strategy is also being applied.

Note that, since parameter **A** in the measurement errors model has been eliminated during ATS/SDTS formulas computations, its value does not affect the chart performance. Sabahno et al. [4] also showed that the larger the value of parameter **B** is, the better the chart performs in the presence of measurement errors. However, unlike the number of multiple measurements (m), only the measurement system determines the value of **B**, not the practitioners.

In this section, we assume that $\theta = (0.2, 0.2, 0.2)$, $\phi = (0.4, 0.4, 0.4)$, $\tau = 1.2$, $\mu_1 = (1.5, 1.5)$, $\mathbf{B} = 2\mathbf{I}$, and m changes from 1 to 10 in each plot.

We also assume that ε varies from $(0.1, 0.1)$ to $(0.3, 0.3)$, $(0.5, 0.5)$ and $(0.8, 0.8)$ in each plot. This analysis is performed for $s = 0$, 1, 2, 4, each used in separate plots. All other design and process parameters value assumptions are as before.

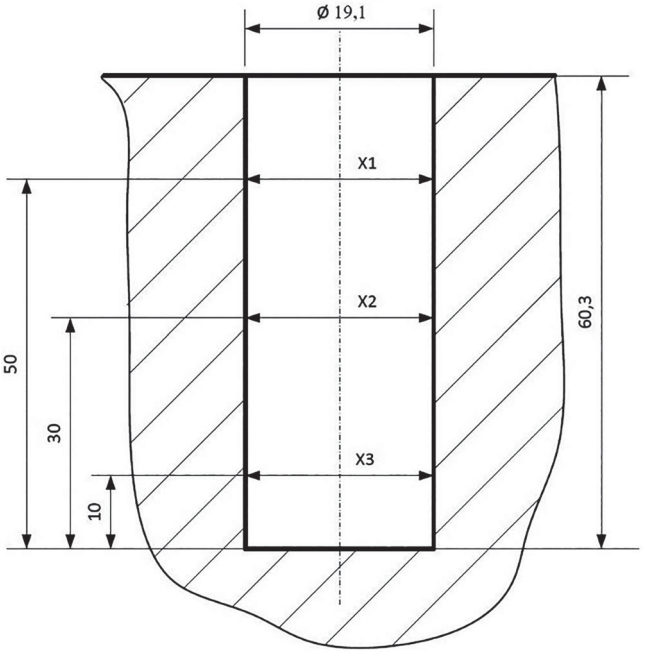

Figure 3. A hole in a plate with three quality characteristics.

The results of this investigation are shown in Figure 2. It is clear that not only multiple measurements will improve the chart performance, but also if one combines it with the skip-sampling strategy, it will further improve the chart performance. However, in all the cases, multiple measurements are only effective up to some number of measurements *m,* and after that, no significant improvement will occur in the chart performance. The larger the measurement errors (ε) are, the more multiple measurements are needed until the chart becomes insensitive to the number of multiple measurements.

7. An illustrative example

To show how the proposed control chart in this paper can be applied in practice, we adopt a real case first introduced by Sabahno et al. [4] by considering measurement errors. Later, Sabahno et al. [5] adopted the same case for an autocorrelated process. In this paper, we will investigate a more realistic scenario that involves both measurement errors and autocorrelation.

A company makes mechanical plates where up to 8 holes can be bored into them by using a CNC drilling machine. It has been decided to measure the holes at $p = 3$ different levels (10mm, 30mm, 50mm) to achieve the required accuracy, see Figure 3.

We use the same process and design parameters values as in Sabahno et al. [4]. The process mean vector is $\mu_0 = (19.0998, 19.0997, 19.0996)$. Because of the measurement system, there are measurement errors in the process and the values for the measurement errors model parameters are obtained as:

$\mathbf{A} = a\mathbf{1}$, $\mathbf{B} = b\mathbf{I}$, and $\mathbf{\Sigma}_\varepsilon = \sigma_\varepsilon^2\mathbf{I}$ with $\hat{a} = -0.0008$, $\hat{b} = 1.0002$ and $\hat{\sigma}_\varepsilon = 0.000629$.

As for the design parameters, we have:

Table 7. Control table: details of 20 samples taken for online process monitoring.

i	η	$\sum n_i$	t_t	$\sum t_i$	M_i	V_i	C_i	UWL_i	UCL_i	Status
1	4	4	110	110	−0.1116	−0.1122	0.1122	1.0514	3.6622	In-control
2	4	8	110	220	−0.2137	0.6476	0.6476	1.0514	3.6622	In-control
3	4	12	110	330	1.0586	1.3763	1.3763	1.0514	3.6622	In-control
4	8	20	10	340	1.0976	2.0859	2.0859	1.0445	2.8228	In-control
5	8	28	10	350	0.0403	1.6172	1.6172	1.0445	2.8228	In-control
6	8	36	10	360	−2.2713	0.8925	2.2713	1.0445	2.8228	In-control
7	8	44	10	370	−0.6311	1.0158	1.0158	1.0445	2.8228	In-control
8	4	48	110	480	−2.1900	1.0903	2.1900	1.0514	3.6622	In-control
9	8	56	10	490	0.5191	1.6261	1.6261	1.0445	2.8228	In-control
10	8	64	10	500	1.2862	1.5167	1.5167	1.0445	2.8228	In-control
11	8	72	10	510	−1.0382	0.9022	1.0382	1.0445	2.8228	In-control
12	4	76	110	620	0.5283	1.1897	1.1897	1.0514	3.6622	In-control
13	8	84	10	630	0.6872	1.3916	1.3916	1.0445	2.8228	In-control
14	8	92	10	640	0.0820	2.6211	2.6211	1.0445	2.8228	In-control
15	8	100	10	650	1.0870	2.8554	**2.8554**	1.0445	**2.8228**	**Out-of-control**
16	8	108	10	660	−0.2421	2.0106	2.0106	1.0445	2.8228	In-control
17	8	116	10	670	0.4224	1.1663	1.1663	1.0445	2.8228	In-control
18	8	124	10	680	−1.1589	0.7211	1.1589	1.0445	2.8228	In-control
19	8	132	10	690	1.9365	1.8396	1.9365	1.0445	2.8228	In-control
20	8	140	10	700	1.0424	1.8662	1.8662	1.0445	2.8228	In-control

$ASI = 60$ *mins*, $ASS = 6$ *holes*, $ATE = 0.005$, $\alpha_1 = 0.0005$, $(n_1, n_2) = (4, 8)$ *holes,* and $t_2 = 10$ *mins*. Using Equations (15, 20-22), we have $UCL_1 = 3.6622$, $UWL_1 = 1.0514$, $\alpha_2 = 0.0095$, $UCL_2 = 2.8228$, $UWL_2 = 1.0445$ and $t_1 = 110$ *mins*.

In addition, due to a recent modification in the sampling system, the sampling intervals within samples, have been considerably reduced and this has caused an autocorrelation. We further assume the following values for the autocorrelation model parameters:

$$\boldsymbol{\Sigma}_{e_0} = \begin{bmatrix} 4.826 \times 10^{-6} & 1.95 \times 10^{-7} & 4.1 \times 10^{-8} \\ 1.95 \times 10^{-7} & 4.275 \times 10^{-6} & -3.63 \times 10^{-7} \\ 4.1 \times 10^{-8} & -3.63 \times 10^{-7} & 5.426 \times 10^{-6} \end{bmatrix},$$

$$\Phi = \begin{bmatrix} 0.25 & 0.04 & 0.22 \\ 0.3 & 0.1 & -0.054 \\ 0.3 & 0.2 & 0.321 \end{bmatrix} \text{ and } \Theta = \begin{bmatrix} 0.136 & -0.151 & 0.11 \\ -0.29 & 0.09 & 0.21 \\ -0.34 & 0.043 & 0.22 \end{bmatrix}.$$

To see how the control scheme works, we shift the mean vector to $\mu_1 = (19.1009, 19.1006, 19.0998)$ and the random noise variance-covariance matrix to

$$\boldsymbol{\Sigma}_{e_1} = \begin{bmatrix} 4.973 \times 10^{-6} & 1.9 \times 10^{-7} & 4.5 \times 10^{-8} \\ 1.9 \times 10^{-7} & 5.25 \times 10^{-6} & -3.69 \times 10^{-7} \\ 4.5 \times 10^{-8} & -3.69 \times 10^{-7} & 6.53 \times 10^{-6} \end{bmatrix}.$$

We then perform the online process monitoring by taking 20 samples from the process by skipping the samples in between ($s = 1$) and by measuring the next ones twice ($m = 2$). By doing so, according to Sections 6.2 and 6.3, we will alleviate the combined effects of both measurement errors and autocorrelation, and also, since we choose the smallest values for s and m, this does not add difficulty in administrating the control chart. According to Table 7 (control table), as well as Figure 4 (control chart), after 650 *mins* and 100 holes measured, the control chart was able to signal at sample No.15 during the first 20 samples.

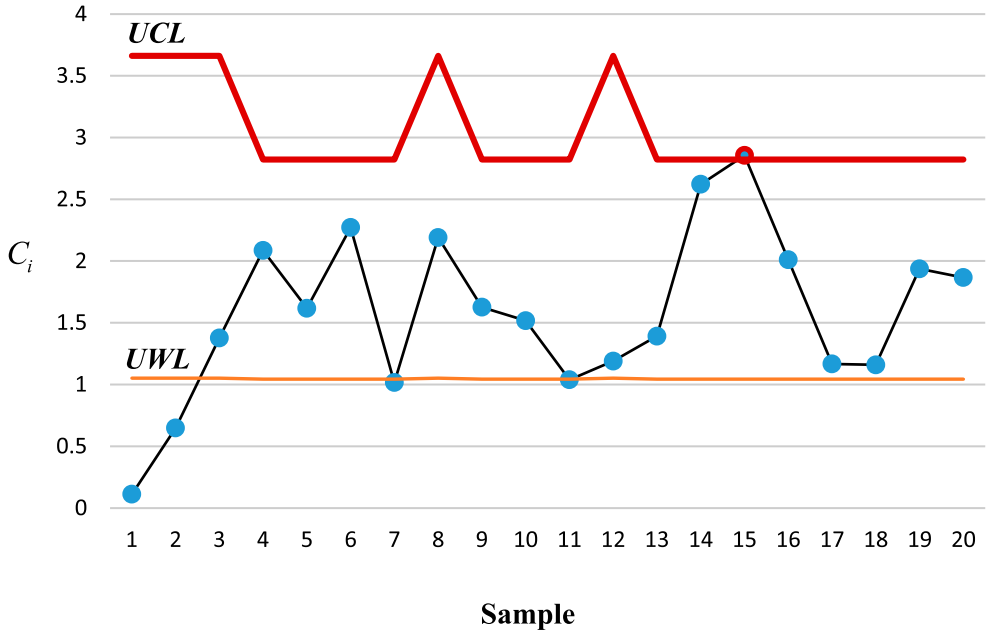

Figure 4. The max-type adaptive control chart for the illustrative example.

8. Concluding remarks and future research

The combined effects of autocorrelation between consecutive observations and measurement errors on a recently developed adaptive VP max-type multivariate control chart were investigated in this paper. To do so, we first developed the control chart by incorporating linearly covariate measurement errors and VARMA autocorrelation models (two of the most common measurement errors and autocorrelation models) into it. In doing so, we also developed a skip-sampling strategy for the ARMA/VARMA models. Then, we added the VP adaptive features to the control scheme. After that, we developed a Markov chain model to compute the control chart's performance measures and we used the average and standard deviation of the time to chart's signal as the performance measures.

Later, for two and four number of quality characteristics ($p = 2, 4$), we performed extensive numerical analyses and simulation studies to investigate the combined effects of autocorrelation and measurement errors and compared them with 'only autocorrelation', 'only measurement errors', and 'no autocorrelation/measurement errors' scenarios under different shift sizes and also under different autocorrelation and measurement errors levels. The result showed that: (i) as the shift in the random noise variance-covariance matrix and/or in the mean vector increases, the chart signals faster, (ii) as the measurement errors increase, the chart signals slower, (iii) the ATS and SDTS values are very close all the time, but the SDTS value is always slightly larger, (iv) in the case the mean shift is not zero, when the value of Φ (AR component) is larger, the chart signals slower and when the Θ value (MA component) is larger, the chart signals faster, however, in the case the measurement errors are available in the process, the above-mentioned rule is not always valid, and, (v) the chart signals faster when there are more quality characteristics.

Next, we used multiple measurements and skip-sampling strategies to reduce the negative effects of measurement errors and autocorrelation, respectively. We used three quality characteristics ($p = 3$) for these analyses. The results of these graphical analyses showed that as the number of skipped samples (s) increases, the chart signals faster. However, the skip-sampling strategy is only effective until some number of skipped samples value (s), and after that, the chart becomes insensitive to the change in the value of s. The larger the value of Φ (the smaller the mean vector shift) is, the more (less) skipped samples are required until the chart becomes insensitive to the number of skipped samples. Moreover, the results showed that not only multiple measurements will improve the chart's performance, but also if combined with the skip-sampling strategy, it will further improve the chart performance. However, multiple measurements too are only effective up to some number of measurements (m), and after that, no significant improvement will occur in the chart's performance. The larger the measurement errors are, the more multiple measurements are needed until the chart becomes insensitive to the m value. Finally, we presented an illustrative real-case industrial example.

For future developments, since the idea of considering the combined effects of measurement errors and autocorrelation is rather new, interested researchers can investigate such an effect on many different 'classical' / 'adaptive', 'univariate' / 'multivariate' and 'single parameter monitoring' / 'simultaneous parameters monitoring' control charts. In addition, investigating other techniques for reducing their negative effects could be another idea for future developments. Moreover, other measurement errors models (such as models with non-constant errors variance, additive Berkson model, multiplicative model, or additive-multiplicative model), as well as other autocorrelation models (such as AR or ARMA models with high orders, non-stationary ARIMA model, non-linear ARCH & GARCH models, or continuous-time Wiener model), in univariate or multivariate cases, might be worth considering by some researchers.

Disclosure statement

No potential conflict of interest was reported by the author(s).

References

[1] Sabahno H, Amiri A, Castagliola P. A new adaptive control chart for the simultaneous monitoring of the mean and variability of multivariate normal processes. Comput Ind Eng. 2021;151. doi:10.1016/j.cie.2020.106524.
[2] Faraz A, Heuchenne C, Saniga E, et al. Double-objective economic statistical design of the VP T^2 control chart: Wald's identity approach. J Stat Comput Simul. 2014;84(10):2123–2137.
[3] Seif A, Faraz A, Saniga E, et al. A statistically adaptive sampling policy to the Hotelling's T^2 control chart: Markov chain approach. Commun Stat-Theory Methods. 2016;45(13):3919–3929.
[4] Sabahno H, Castagliola P, Amiri A. A variable parameter multivariate control chart for simultaneous monitoring of the process mean and variability with measurement errors. Qual Reliab Eng Int. 2020;36(4):1161–1196.
[5] Sabahno H, Castagliola P, Amiri A. An adaptive variable-parameters scheme for the simultaneous monitoring of the mean and variability of an autocorrelated multivariate normal process. J Stat Comput Simul. 2020;90(8):1430–1465.
[6] Lee MH, Khoo MBC. Multivariate synthetic |S| control chart with variable sampling interval. Commun Stat - Simul Comput. 2015;44(4):924–942.

[7] Sabahno H, Amiri A, Castagliola P. Optimal performance of the variable sample sizes Hotelling's T^2 control chart in the presence of measurement errors. Qual Technol Quant Manag. 2018;16(5):588–612.
[8] Sabahno H, Amiri A, Castagliola P. Evaluating the effect of measurement errors on the variable sampling intervals Hotelling T^2 control charts. Qual Reliab Eng Int. 2018;34:1785–1799.
[9] Yeh A, Lin D, Zhou H, et al. A multivariate exponentially weighted moving average control chart for monitoring process variability. J Appl Stat. 2003;30(5):507–536.
[10] Reynolds Jr MR, Gyo-Young C. Multivariate control charts for monitoring the mean vector and covariance matrix. J Qual Technol. 2006;38(3):230–253.
[11] Khoo MBC. A new bivariate control chart to monitor the multivariate process mean and variance simultaneously. Qual Eng. 2005;17:109–118.
[12] Zhang J, Li Z, Wang Z. A multivariate control chart for simultaneously monitoring process mean and variability. Comput Stat Data Anal. 2010;54(10):2244–2252.
[13] Wang K, Yeh AB, Li B. Simultaneous monitoring of process mean vector and covariance matrix via penalized likelihood estimation. Comput Stat Data Anal. 2014;78(1):206–217.
[14] Reynolds Jr MR, Kim K. Multivariate control charts for monitoring the process mean and variability using sequential sampling. Seq Analy: Design Methods Appl. 2007;26:283–315.
[15] Reynolds Jr MR, Cho GY. Multivariate control charts for monitoring the mean vector and covariance matrix with variable sampling intervals. Seq Analy: Design Methods Appl. 2011;30:1–40.
[16] Sabahno H, Khoo MBC. A multivariate adaptive control chart for simultaneously monitoring of the process parameters. Commun Stat - Simul Comput. 2022. doi:10.1080/03610918.2022.2066695.
[17] Sabahno H, Amiri A. Simultaneous monitoring of the mean vector and covariance matrix of multivariate multiple linear profiles with a new adaptive Shewhart-type control chart. Qual Eng. 2023. doi:10.1080/08982112.2022.2164725.
[18] Jalilibal Z, Amiri A, Khoo MBC. A literature review on joint control schemes in statistical process monitoring. Qual Reliab Eng Int. 2022;38(6):3270–3289.
[19] Linna KW, Woodall WH. Effect of measurement error on Shewhart control charts. J Qual Technol. 2001;33(2):213–222.
[20] Linna KW, Woodall WH, Busby KL. The performance of multivariate control charts in the presence of measurement error. J Qual Technol. 2001;33(3):349–355.
[21] Chattinnawat W, Bilen C. Performance analysis of Hotelling T^2 under multivariate inspection errors. Qual Technol Quant Manag. 2017;14(3):249–268.
[22] Zaidi FS, Castagliola P, Tran KP, et al. Performance of the Hotelling T^2 control chart for compositional data in the presence of measurement errors. J Appl Stat. 2019;46(14):2583–2602.
[23] Huwang L, Hung Y. Effect of measurement error on monitoring multivariate process variability. Stat Sin. 2007;17(2):749–760.
[24] Dizabadi K, Shahrokhi A, Maleki M, et al. On the effect of measurement error with linearly increasing-type variance on simultaneous monitoring of process mean and variability. Qual Reliab Eng Int. 2016;32(5):1693–1705.
[25] Ghashghaei R, Bashiri M, Amiri A, et al. Effect of measurement error on joint monitoring of process mean and variability under ranked set sampling. Qual Reliab Eng Int. 2016;32(8):3035–3050.
[26] Maleki MR, Amiri A, Castagliola P. Measurement errors in statistical process monitoring: a literature review. Comput Ind Eng. 2017;103:316–329.
[27] Kalgonda AA, Kulkarni SR. Multivariate quality control chart for autocorrelated processes. J Appl Stat. 2004;31:317–327.
[28] Jarrett JE, Pan X. Monitoring variability and analyzing multivariate autocorrelated processes. J Appl Stat. 2007;34(4):459–469.
[29] Vanhatalo E, Kulahci M. The effect of autocorrelation on the Hotelling T^2 control chart. Qual Reliab Eng Int. 2015;31(8):1779–1796.
[30] Leoni RC, Costa AFB, Sampaio NAS, et al. A geometric approach to illustrate the autocorrelation effect in T^2 control chart of Hotelling. Appl Math (Irvine). 2015;5(2):39–47.

[31] Dargopatil P, Ghute V. New sampling strategies to reduce the effect of autocorrelation on the synthetic T^2 chart to monitor bivariate process. Quality Reliability Engineering International. 2018;34:1–17.
[32] Rahimi SB, Amiri A, Ghashghaei R. Simultaneous monitoring of mean vector and covariance matrix of multivariate simple linear profiles in the presence of within profile autocorrelation. Commun Stat-Simul Comput. 2021;50(6):1791–1808.
[33] Rahimi SB, Amiri A, Khoo MBC, et al. Simultaneous monitoring of mean vector and covariance matrix of auto correlated multivariate multiple linear profiles. Qual Reliab Eng Int. 2022;38(7):3513–3542.
[34] Costa AFB, Castagliola P. Effect of measurement error and autocorrelation on the chart. J Appl Stat. 2011;38(4):661–673.
[35] Franco BC, Castagliola P, Celano G, et al. A new sampling strategy to reduce the effect of autocorrelation on a control chart. J Appl Stat. 2014;41(7):1408–1421.
[36] Franco BC, Castagliola P, Celano G, et al. Economic design of Shewhart control charts for monitoring autocorrelated data with skip sampling strategies. Int J Prod Econ. 2014;151:121–130.
[37] Ma X, Zhang L, Hu J, et al. A model-free approach to reduce the effect of autocorrelation on statistical process control charts. J Chemom. 2018;32(12):1–24.
[38] Yang SF, Yang CM. Effects of imprecise measurement on the two dependent processes control for the autocorrelated observations. Int J Adv Manufact Tech. 2005;26:623–630.
[39] Xiaohong L, Zhaojun W. The CUSUM control chart for the autocorrelated data with measurement error. Chinese Journal of Applied Probability. 2009;25(5):461–474.
[40] Shongwe SC, Malela-Majika JC, Castagliola P. The new synthetic and runs-rules schemes to monitor the process mean of autocorrelated observations with measurement errors. Commun Stat - Theory Methods. 2021;50(24):5806–5835.
[41] Beydaghi H, Amiri A, Jalilibal Z, et al. On the effect of measurement errors and auto-correlation on the performance of Hotelling's T2 control chart. J Indus Syst Eng. 2021;13(3):193–215.